ELECTRONIC TRANSPORT IN MAGNETIC TUNNEL JUNCTION: A DISCUSSION OF THE ELECTRON-MAGNON-PHOTON COUPLING

BY YANG XIAO AND HONG GUO

One of the most useful spintronics phenomena [1] is the tunnel magnetoresistance (TMR) observed in magnetic tunnel junctions (MTJs). An MTJ is a tunnel structure where two ferromagnetic layers (FM) sandwich a thin insulating barrier. The tunneling current $I_{\uparrow\uparrow}$ is large when magnetic moments of the two FM layers are in parallel configuration (PC, $\uparrow\uparrow$), and $I_{\uparrow\downarrow}$ is small when they are antiparallel (APC, $\uparrow\downarrow$). Due to this binary nature, MTJs have become the elementary unit of the magnetic random access memory (MRAM) technology [2,3]. From a practical point of view, extensive research has focused on producing MTJs having a large TMR ratio [4–6] which is defined as $(I_{\uparrow\uparrow} - I_{\uparrow\downarrow}) / I_{\uparrow\downarrow}$; improving switching capability between PC and APC using advanced techniques based on spin transfer torque [7], and improving the material properties etc.

Being very sensitive to external magnetic field, MTJs have been used as field sensors, e.g., read sensors in hard drives [4–6]. Due to suitable energetics, MTJs have recently been applied in microwave sensing [8] and even microwave imaging by phase-sensitive detection techniques [9]. Spintronics-based microwave technology is a very exciting new direction of nanotechnology whose principle is totally different from the conventional radar approach. When a magnetic system (e.g., an MTJ) is subjected to microwave radiation, complicated spin dynamics may occur which influences spin-polarized charge transport in the system, and microwave sensing is achieved by electrical detection of the changes of the transport signal. Microwave rectification [10–12], e.g. the generation of a DC electric current by magnetization dynamics, is such a transport phenomenon characterized by charge or spin currents. It is now generally accepted that several physical mechanisms including spin rectification [11], spin pumping [10], spin torque diode effects [12],

etc., can co-exist in a device to produce the observed radio-frequency sensing data in metal spintronics.

Fig. 1 shows a typical model of MTJs where the left/right leads are FM metals (for instance Fe) and the device region is a very thin insulating tunnel barrier (for instance YIG). In an MTJ, electrons are driven to quantum mechanically tunnel through by an external bias voltage V. In a microwave rectification experiment, a static magnetic field $\vec{H}_{ext}$ is applied to induce spin precession around it. The precession is eventually damped out by various relaxation processes in the material. A microwave field with wave vector $\vec{k}$ can be applied to deflect the spins from the direction of $\vec{H}_{ext}$ and to maintain a stable spin precession by overcoming the damping processes. Since resistance oscillates with the orientation and magnitude of the magnetization due to various physical mechanisms, the oscillating current and oscillating resistance produce an AC voltage that has a DC component across the sample. Such a rectification was experimentally demonstrated in Ref. [13]. Reversely, by detecting the DC signal, the device acts as a microwave sensor.

Fig. 1 Theoretical model of an MTJ. Two leads are biased with a voltage V. The external magnetic field H_{ext} and a microwave are applied. The spin wave is shown in central region.

SUMMARY

We present a pedagogical discussion on electron transport in magnetic tunnel junctions under the electron-magnon-photon interaction.

Yang Xiao <yxiao263@gmail.com>, College of Science, Nanjing University of Aeronautics and Astronautics, Nanjing 210016, China and Centre for the Physics of Materials and Department of Physics, McGill University, Montreal, QC H3A 2T8

and

Hong Guo <guo@physics.mcgill.ca>, Centre for the Physics of Materials and Department of Physics, McGill University, Montreal, QC H3A 2T8

In the device model of Fig. 1, conduction electrons, precessing magnetic moments, and electromagnetic fields are all present[1]. The collective motion of the magnetic moments is a spin wave and its quantize version is a magnon. Similarly, the quantum of the electromagnetic field is a photon. In principle, quantum transport in such systems involves interactions between electrons, magnons and photons, and the outcome can be quite complicated depending on the coupling strengths between each pair of them. It is the purpose of this article to present a pedagogical discussion of this coupling and its implication to quantum transport. Our discussion is summarized from the outcome of rigorous mathematical derivations using the Keldysh nonequilibrium Green's function (NEGF) formalism [14], which is summarized elsewhere [15].

The rest of this article is organized as follows. The next section presents a device model as the example for discussion. In the section entitled "*Boson Assisted Transport Processes*", the well-known inelastic tunneling and boson-assisted tunneling are discussed. Depending on the coupling strength of magnon-photon interaction, weak coupling and strong coupling regimes are recognized and discussed in the sections entitled "*Weak Coupling*" and "*Strong Coupling*" respectively. Finally, the section entitled "*Perspective*" presents a short conclusion and discussion on future perspectives.

THE DEVICE MODEL

The Hamiltonian of the device model in Fig. 1 can be written in the following form,

$$H = H_\alpha + H_d + H_t \tag{1}$$

where $H_\alpha = \sum_{\alpha,k} \epsilon_{\alpha,k} d^\dagger_{\alpha,k} d_{\alpha,k}$ is the Hamiltonian of the left and right leads of the device ($\alpha = L,R$), k indicates the quantum states of the leads, $d^\dagger_{\alpha,k}(d_{\alpha,k})$ are the creation (annihilation) operators of electrons in lead α, and $\epsilon_{\alpha,k}$ is the energy of the electrons. The simplest form of the Hamiltonian for the central region of the device (see Fig. 1) is,

$$
\begin{aligned}
H_d = &\sum_e \epsilon_e c^\dagger_e c_e + \sum_p \epsilon_p a^\dagger_p a_p + \sum_m \epsilon_m b^\dagger_m b_m \\
&+ \sum_{e,p} g_{ep} c^\dagger_e c_e \left[a^\dagger_p + a_p\right] + \sum_{e,m} g_{em} c^\dagger_e c_e \left[b^\dagger_m + b_m\right] \\
&+ \sum_{m,p} g_{mp} \left[a^\dagger_p b_m + a_p b_m\right],
\end{aligned}
\tag{2}
$$

where the first three terms represent energies of bare electrons, photons and magnons; the last three terms represent electron-

photon, electron-magnon and magnon-photon interactions. $c^\dagger_e(c_e)$, $a^\dagger_p(a_p)$ and $b^\dagger_m(b_m)$ are the creation (annihilation) operators of electron, photon and magnon with eigen-energy ϵ_e, ϵ_p and ϵ_m, respectively. g_{ep}, g_{em} and g_{mp} represent the coupling strength of electron-photon, electron-magnon and magnon-photon interactions. Here the electron-electron interaction is neglected for simplicity. Finally, the central region of the device is coupled to the leads by the Hamiltonian H_t in the familiar form [14] of $H_t \sim d^\dagger_k c_e$. In the above model, the left and right leads play the role of source and drain for electrons traversing the central region.

The electric current flowing from the left lead to the device can be derived by the standard Green's function theory [14,16],

$$J_L = \frac{e}{\hbar} \int \frac{dE}{2\pi} \mathrm{Tr}(\Sigma^<_L G^> - \Sigma^>_L G^<), \tag{3}$$

where e and $\hbar$ are elementary charge and reduced Planck constant. $\Sigma^{<>}_L$ is the lesser/greater self-energy of the leads which reflects the electron scattering rates from the leads to the central part of the device. $G^{<>}$ is the lesser/greater Green's function of the device which describes the electron/hole density matrix. The physical meaning of Eq. (3) is clear: $\Sigma^<_L G^>$ and $\Sigma^>_L G^<$ represent the forward and backward tunnelling current and thus the difference constitutes the net current in the left lead. The Green's function G is the most important quantity in our theory which can be calculated by a perturbation-like series expansion [17],

$$
\begin{aligned}
G(t - t') = &\sum_{n=0}^{\infty} \frac{(-i)^{n+1}}{n!} \int_{-\infty}^{\infty} dt_1 \cdots \int_{-\infty}^{\infty} dt_n \\
&\times \langle \phi | \mathrm{T} c(t) V(t_1) \cdots V(t_n) c^\dagger(t') | \phi \rangle,
\end{aligned}
\tag{4}
$$

where $V(t)$ is the various interactions such as those appearing in Eq. (2), $|\phi\rangle$ is the ground state, T is time-ordering operator. Although the Green's function consists of infinite terms in general, we shall only consider the lowest order terms. The $n = 0$ term in Eq. (4) is the Green's function in the absence of any interaction; the $n = 2$ and $n = 4$ terms will be emphasized in the sections which follow.

For simplicity of the discussion, we shall consider a quantum dot model for the center part of the device having one energy level ϵ_e, photons with a single energy ϵ_p, and a single mode in the magnon spectrum. As a result, the summations over the quantum indices in Eq. (2) are dropped. In addition, the left/right leads and the lead-device coupling are described by interaction-free electron reservoirs. For more details of the calculation of J_L, we refer interested readers to Ref. [18].

---

1. The model in Fig. 1 is somewhat different from an usual MTJ which has non-magnetic spacer where magnons are excited at the proximity region between the ferromagneic electrodes and the spacer. To focus on magnon-related tunneling physics while avoiding complications of proximity effect, here we consider a magnetic insulator as the spacer. This does not affect the tunneling nature of the usual MTJ.

BOSON-ASSISTED TRANSPORT PROCESSES

Since magnons and photons are bosons, we start by discussing quantum tunneling in MTJ assisted by these boson fields. It has been well understood, both theoretically and experimentally, that boson-like particles can enhance electron transmission [19]. From a theoretical point of view, substituting the interaction $V = g_{ep}c^{\dagger}c[a^{\dagger} + a] + g_{em}c^{\dagger}c[b^{\dagger} + b]$ of Eq. (2) into Eq. (4), the $n = 2$ terms of the Green's function reflect electron scattering by the one-boson processes (magnon or photon) with the physical mechanism depicted in Fig. 2(a,b). Fig. 2(a) is for the simple case of excitation where an electron enters the central device region from the left lead, it absorbs a boson (e.g.,

magnon or photon), gets excited to high enough energy that allows it to exit to the right lead. For this situation, direct tunneling is clearly impossible at zero external bias. Fig. 2(b) is for the bias situation where direct tunneling is possible but can be further assisted by emitting bosons to open up more transmission channels for exiting the device. This process leads to the well-known inelastic tunneling spectroscopy [20] (IETS). The boson-assisted processes depend on boson frequency and wave vector, hence the assisted tunneling spectra can be used to detect the frequency (energy) of the bosons: IETS has already been employed to detect the mode frequency of phonons and magnons in a number of experiments [21]. Fig. 2(d) and (e) show inelastic current (I_{ine}) arising from the
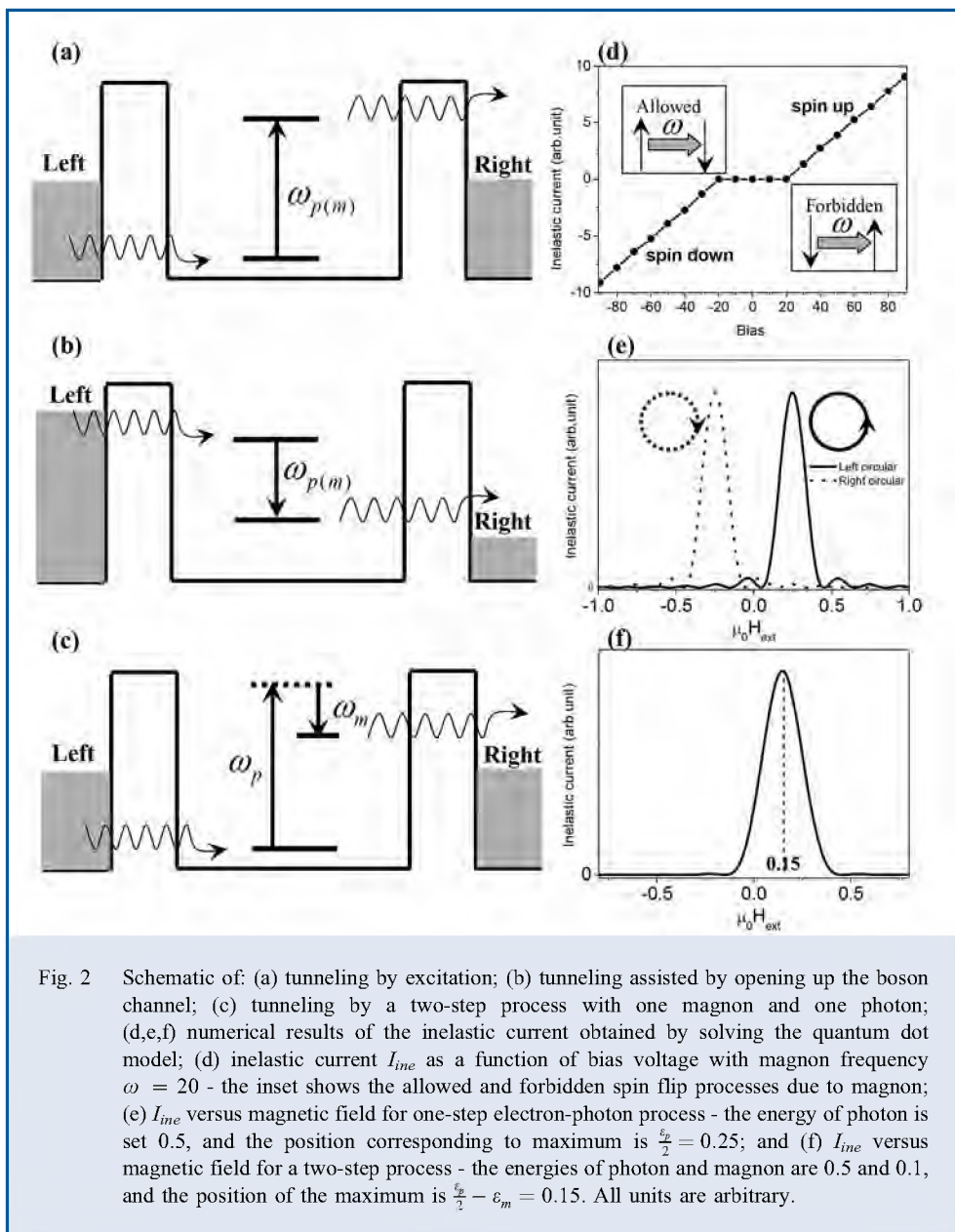
Fig. 2   Schematic of: (a) tunneling by excitation; (b) tunneling assisted by opening up the boson channel; (c) tunneling by a two-step process with one magnon and one photon; (d,e,f) numerical results of the inelastic current obtained by solving the quantum dot model; (d) inelastic current I_{ine} as a function of bias voltage with magnon frequency $\omega = 20$ - the inset shows the allowed and forbidden spin flip processes due to magnon; (e) I_{ine} versus magnetic field for one-step electron-photon process - the energy of photon is set 0.5, and the position corresponding to maximum is $\frac{\varepsilon_p}{2} = 0.25$; and (f) I_{ine} versus magnetic field for a two-step process - the energies of photon and magnon are 0.5 and 0.1, and the position of the maximum is $\frac{\varepsilon_p}{2} - \varepsilon_m = 0.15$. All units are arbitrary.

magnon- or photon-assisted tunneling. The numerical curves were obtained by calculations of the quantum dot model. In IETS, below a threshold voltage only direct tunneling can occur due to the quantum nature of the boson. Above this threshold voltage, the assisted tunneling starts to contribute to the current, see Fig. 2(d). The value of the threshold voltage gives a direct measure of the boson energy or frequency. The IETS of magnon or photon can be made possible by varying the magnetic field instead of the bias voltage, as shown in Fig. 2(e). Moreover, due to the fact that magnon or circularly-polarized photon holds one spin angular momentum, the tunneling current is spin polarized when bias voltage or magnetic field is changing, as shown in Fig. 2(d) and (e).

The processes in Fig. 2(a) and (b) involve absorption or emission of a single boson. For the MTJ device in Fig. 1, there are two kinds of bosonic particles, magnon and photon. It is interesting to understand how the two bosonic particles influence electronic transport together. In particular, for the microwave sensing with MTJs, electron-magnon, electron-photon and magnon-photon couplings occur at the same time. In general, the coupling strength varies with the specific details of the MTJ device and material. Depending on the coupling strength of the magnon-photon interaction, the device can be characterized as being in the "weak coupling regime" or "strong coupling regime".

WEAK COUPLING

The direct coupling between magnon and photon, i.e. the parameter g_{mp} in Eq. (2), is usually very small and thus can be omitted [22]. This is the weak coupling regime. To first order ($n = 2$) of the electron-boson coupling strength, one obtains magnon-assisted tunneling and/or photon-assisted tunneling respectively- the well-known physics was discussed in the last section (Fig. 2(a) and (b)).

The second order treatment can be worked out by the Green's function formalism to reveal a two-step sequential tunneling process. The basic idea is to consider the $n = 4$ terms in Eq. (4). The $n = 4$ terms consist of three terms describing electron scattering with two magnons, with two photons, and with one magnon plus one photon. Apart from the two-boson nature, the former two terms have nothing new compared with the simple physics described in the last section. The last term, shown in Fig. 2(c), depicts where the incoming electron first absorbs a photon and then emits a magnon. Based on quantum dot calculation shown in Fig. 2(f), one could see that I_{ine} of such a two-step sequential process is on resonance at the magnetic field determined by the frequency difference between the magnon and photon. The reverse process is theoretically allowed but is not dominant for low-intensity microwave fields. Although such a two-step photon-magnon process has not been observed experimentally so far, its *phonon* counter-

part – the two-step photon-phonon process, has been subjected to extensive investigations both theoretically and experimentally in the semiconductor literature [15].

STRONG COUPLING

A strong coupling between magnon and photon is perhaps the most interesting situation. As mentioned above, for a long time the direct coupling between magnon and photon has been neglected. Experimentally, this was due to the achievable quality factor (Q) of cavity and low-spin density of magnetic materials which lead to very small coupling g_{mp}. Thanks to advances in fabrication techniques of high-Q cavity and pure single-crystalline magnetic insulator YIG, strong coupling via magnetic dipole between photon and magnon has been realized recently [23–26]. The well-established systems – consisting of the cavity and ferromagnetic resonance (FMR) set-up, enable strong and even ultra-strong coupling with strength up to a few GHz. Such a coupled system is usually called magnon polariton. Recently, magnon polariton has been observed experimentally at both ultralow temperature (0.01 K) and room temperature [23–26]. The co-existence at low and high temperatures has led one to consider the quantum and classical nature of the processes [see the article "*Dawn of cavity spintronics*" by C.M. Hu in the same issue].

For strong coupling, the theoretical treatment of Eq. (2) is more complicated than that for weak coupling since all three coupling parameters must be included. Note that the coupling strength of electron-photon/magnon can be ~ 100 meV while the magnon-photon coupling can be up to ~ 0.01 meV, hence the magnon-photon coupling can still be treated perturbatively. A qualitative picture can be obtained as follows. We first solve the magnon and photon Hamiltonian $H_{mp} = \epsilon_p a^\dagger a + \epsilon_m b^\dagger b + g_{mp}[a^\dagger b + ab^\dagger]$ with the Bogoliubov transformation $a = A\cos\theta + B\sin\theta$ and $b = B\cos\theta - A\sin\theta$. The Hamiltonian is then diagonalized, $H_{mp} = \epsilon^+ A^\dagger A + \epsilon^- B^\dagger B$, by adjusting the parameter θ. Substituting the above transformation into the remaining terms of Eq. (2), we obtain a reduced polariton Hamiltonian,

$$H_d = \epsilon_e c^\dagger c + \sum_{d=A,B} \left\{ \epsilon^\pm d^\dagger d + g_{e\pm} c^\dagger c [d^\dagger + d] \right\}, \qquad (5)$$

where $d = A(B)$ are operators for upper(lower) branches of polariton with eigen-energy $\epsilon^\pm$ and interaction strength $g_{e+} = g_{ep}\cos\theta - g_{em}\sin\theta$ and $g_{e-} = g_{ep}\sin\theta + g_{em}\cos\theta$ respectively.

The polariton Hamiltonian Eq. (5) indicates that the magnon-photon interaction produces magnon polariton with an upper and a lower branch schematically shown in Fig. 3(a) where, roughly, the photon, magnon and magnon polariton are thought of as harmonic oscillators. The dispersion of upper and lower branches, i.e., $\epsilon\pm$, are shown in Fig. 3(b). Due to for-mations of the magnon polariton, the electron-magnon and electron-photon interaction strengths are renormalized to give
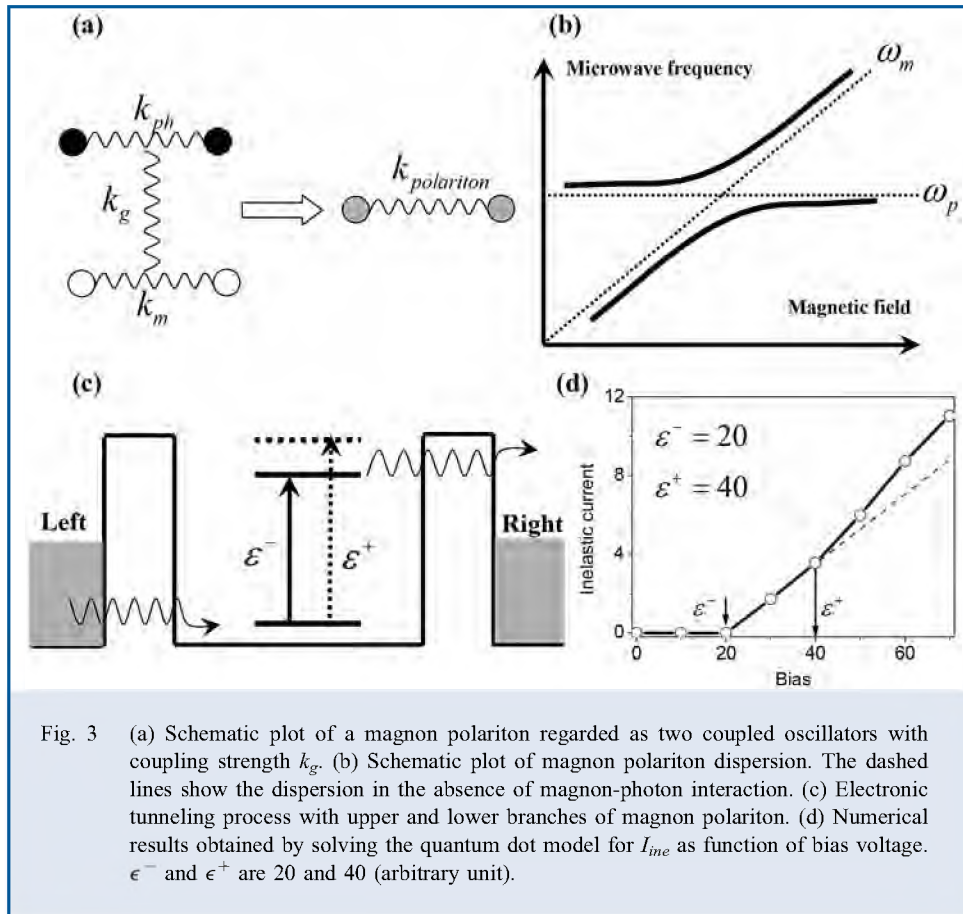
Fig. 3   (a) Schematic plot of a magnon polariton regarded as two coupled oscillators with coupling strength k_g. (b) Schematic plot of magnon polariton dispersion. The dashed lines show the dispersion in the absence of magnon-photon interaction. (c) Electronic tunneling process with upper and lower branches of magnon polariton. (d) Numerical results obtained by solving the quantum dot model for I_{ine} as function of bias voltage. ϵ^- and ϵ^+ are 20 and 40 (arbitrary unit).

the interaction strengths between the electron and upper/lower branches of magnon polariton.

Having understood the elementary excitations in the device scattering region, new features of electron tunneling are expected due to the presence of magnon polariton. First, from the Bogoliubov transformation, we have $[A, A^\dagger] = 1$ and $[A, B^\dagger] = 0$, which indicates that polariton obeys bosonic statistics. Consequently, a new tunneling behavior is expected, i.e., polariton-assisted tunneling in MTJs where electron transitions take place for both the upper and lower branches as shown in Fig. 3(c). Therefore, as seen in Fig. 3(d) which plots the numerical curves obtained by solving the quantum dot model, I_{ine} will be enhanced at both ϵ^+ and ϵ^- as bias voltage increases. Second, the energy of a polariton can be tuned by the external magnetic field and microwave frequency. Such tunability adds extra degrees of freedom into electronic transport in addition to bias and gate voltage used in conventional devices. Third, an asymmetry appears in the tunneling current for the upper and lower branches. Based on Eqs. (3), (4) and (5), the inelastic tunneling current is proportional to the square of electron-boson coupling strength ($n = 2$). Due to different strengths for coupling to the upper

and lower polariton branches, the tunneling current develops an asymmetric structure. This feature could be used to detect the existence of magnon polariton in transport measurements. Further details of these transport features will be presented elsewhere [15].

PERSPECTIVE

In this short article we have presented a paragogical discussion of the tunneling physics induced by the electron-magnon-photon interaction which is realized in microwave-irradiated MTJ devices. For the two-step tunneling, an important task is to make proper connections between theoretical results and experimental measurements. For magnon polariton, there is a need for a theoretical framework to calculate charge current and spin current in a strong coupling regime. Recently, spin current observed in a spin-pumping experiment in the strong coupling regime has been reported by Bai et al. [23]. In theory, the inclusion of a magnon-photon interaction produces new self-energy terms which make the time-dependent problem more difficult to solve. Another important question is how spin current varies when nonclassical states of photons are used. If a Fock state or squeezed state of photon is prepared

in a magnon polariton experiment successfully, the quantum nature of magnon polariton may be recognized without ambiguity. A new theoretical development is desired to predict the transport of spin current arising from such a nonclassical light. We wish to report these developments in the near future.

REFERENCES

1. S.A. Wolf *et al.*, "Spintronics: a spin-based electronics vision for the future", *Science*, **294**, 1488 (2001).
2. S.S.P. Parkin *et al.*, "Exchange-biased magnetic tunnel junctions and application to nonvolatile magnetic random access memory", *J. Appl. Phys.*, **85**, 5828 (1999).
3. S. Tehrani *et al.*, "High density submicron magnetoresistive random access memory", *J. Appl. Phys.*, **85**, 5822 (1999).
4. S.S.P. Parkin *et al.*, "Giant tunnelling magnetoresistance at room temperature with MgO (100) tunnel barriers", *Nat. Mater.*, **3**, 862 (2004).
5. S. Yuasa *et al.*, "Giant room-temperature magnetoresistance in single-crystal Fe/MgO/Fe magnetic tunnel junctions", *Nat. Mater.*, **3**, 868 (2004).
6. S. Ikeda *et al.*, "Tunnel magnetoresistance of 604% at 300K by suppression of Ta diffusion in CoFeB/MgO/CoFeB pseudo-spin-valves annealed at high temperature", *Appl. Phys. Lett.*, **93**, 082508 (2008).
7. J.C. Slonczewski, "Current-driven excitation of magnetic multilayers", *J. Magn. Magn. Mater.*, **159**, L1 (1996); L. Berger, "Emission of spin waves by a magnetic multilayer traversed by a current", *Phys. Rev.*, B **54**, 9353 (1996).
8. L. Fu *et al.*, "Microwave holography using a magnetic tunnel junction based spintronic microwave sensor", *J. Appl. Phys.*, **117**, 213902 (2015).
9. Z.X. Cao *et al.*, "Nondestructive two-dimensional phase imaging of embedded defects via on-chip spintronic sensor", *Appl. Phys. Lett.*, **100**, 252406 (2012).
10. Y. Tserkovnyak *et al.*, "Nonlocal magnetization dynamics in ferromagnetic heterostructures", *Rev. Mod. Phys.*, **77**, 1375 (2005).
11. Y.S. Gui *et al.*, "Realization of a room-temperature spin dynamo: the spin rectification effect", *Phys. Rev. Lett.*, **98**, 107602 (2007).
12. A.A. Tulapurkar *et al.*, "Spin-torque diode effect in magnetic tunnel junctions", *Nature*, **438**, 339 (2005).
13. Y.S. Gui *et al.*, "High sensitivity microwave detection using a magnetic tunnel junction in the absence of an external applied magnetic field", *Appl. Phys. Lett.*, **106**, 152403 (2015).
14. H. Haug and A. Jauho, *Quantum kinetics in transport and optics of semiconductors*, Spinger, 1997.
15. Y. Xiao *et al.*, in preparation.
16. S. Datta, *Electronic transport in mesoscopic systems*, Cambridge University Press, 1995.
17. G.D. Mahan, *Many particle physics*, Kluwer, 2000.
18. A. Jauho *et al.*, "Time-dependent transport in interacting and noninteracting resonant-tunneling systems", *Phys. Rev.*, B **50**, 5528 (1994).
19. N.A. Pradhan *et al.*, "Vibronic spectroscopy of single C60 molecules and monolayers with the STM", *J. Phys. Chem.*, B **109**, 8513 (2005).
20. B.C. Stipe *et al.*, "Single-molecule vibrational spectroscopy and microscopy", *Science*, **280**, 1732 (1998).
21. D. Tsui *et al.*, "Multiple magnon excitation in NiO by electron tunneling", *Phys. Rev. Lett.*, **27**, 1729 (1971).
22. P.A. Fleury *et al.*, "Scattering of light by one- and two-magnon excitations", *Phys. Rev.*, **166**, 514 (1968).
23. L. Bai *et al.*, "Spin pumping in electrodynamically coupled magnon-photon systems", *Phys. Rev. Lett.*, **114**, 227201 (2015).
24. X. Zhang *et al.*, "Strongly coupled magnons and cavity microwave photons", *Phys. Rev. Lett.*, **113**, 156401 (2014).
25. Y. Tabuchi *et al.*, "Hybridizing ferromagnetic magnons and microwave photons in the quantum limit", *Phys. Rev. Lett.*, **113**, 083603 (2014).
26. H. Huebl *et al.*, "High cooperativity in coupled microwave resonator ferrimagnetic insulator hybrids", *Phys. Rev. Lett.*, **111**, 127003 (2013).